Improvement in the Signal-to-Noise Ratio in the One-Dimensional Image I.

Joy Nichols-Bohlin

Astronomy Programs
Computer Sciences Corporation

Introduction

Evidence that proper alignment of the ITF with the science data image improves the signal-to-noise ratio of the two-dimensional data by factors of 1.4 - 2.5 has been presented at previous meetings (Nichols-Bohlin 1988). However, further steps in the IUESIPS processing which resample the data to a uniform wavelength space prior to the extraction of the spectral data may significantly reduce the benefits gained from proper treatment of the two-dimensional image. More importantly, beam-pulling effects, still not well understood, may also reduce the benefit.

To better understand the improvement that may be possible in the one-dimensional spectral data, due to proper alignment of the ITF with the data image, two types of analysis have been explored. In the first case, an attempt has been made to quantify the improvement in signal-to-noise ratio by comparing the improvement achieved with flat-field data to that achieved with the extracted spectral data. In the second case, selected sets of spectral data have been processed using both explicit geometric correction and production processing techniques (implicit geometric correction) and presented as comparative plots for the purpose of visual comparison.

Flat-field Pseudo-Spectra vs. Actual Stellar Data

Three images were chosen for this analysis. SWP 25069 is a 100% UV-Flood image actually used in the construction of the SWP ITF2. SWP 26437 is also a 100% flat-field image, but one taken about 6 months after the SWP ITF2. Finally, SWP 27005 is a low dispersion image of HD 60753 with a long exposure of sky background added to the image at the time of exposure, taken 3 months after SWP 26437. The high background of this latter image allowed the reseau marks to be automatically located as in the flat-field images, and thus the image to be explicitly geometrically corrected. All three images were processed two ways. First, for each image the reseau marks were located automatically, the image geometrically corrected, and the ITF applied, providing a photometrically and geometrically corrected image. Then the spectral data were extracted. In the case of the flat field images, the usual spectral extraction software was used, creating a pseudo-spectrum. Secondly, the images were processed using current production processing software, which employs an implicit geometric correction using predicted reseau positions which are based on time and temperature of the instrument.

We had previously determined the improvement in the signal-to-noise (S/N) ratio for SWP 25069 when explicit geometric correction was used compared to the production processing method of implicit geomtric correction (Nichols-Bohlin, this issue). Thus, we can now compare the improvement in the extracted spectral data to the improvement in the two-dimensional image previously determined. The S/N ratio improvement factor for the two-dimensional image was determined by calculating the mean flux and standard deviation in each 12x12 pixel box in four large areas of the image. Each of the four mutually exclusive areas is the largest possible square lying entirely inside the target ring, with one corner at the center of the image. The areas are numbered 1,2,3 and 4 for the upper left, upper right, lower left and lower right portions of the image. The S/N ratio determined for each large area is then the average S/N ratio of the small boxes. The improvement in S/N ratio for "Area 1" of the photometrically corrected image (the area in which the majority of the SWP spectral data fall for low dispersion images) was a factor of 2.33 for this image.

Figure 1 shows the ratio of the S/N ratios for the gross spectral data of the explicit geometric correction to the implicit geometric correction. The S/N ratios have been calculated in 6 Å bins. Clearly, the improvement in the spectral data is not as great for the extracted spectral data as reported for the two-dimensional image. While for some isolated bins the improvement is dramatic (factors of 4-8), the mean improvement is between 1.8 and 2. The improvement is less at the longer wavelengths, which fall in the portion of the camera that is inherently smoother, probably due to a defocusing phenomenon. Figure 2 represents the same information as Figure 1, but for the flat-field image SWP 26437. We have not previously quantified the S/N ratio for the two-dimensional image for this image. Remarkably, the improvement in the S/N ratio achieved by using explicit geometric correction (and thus presumably more accurately aligning the ITF with the data image) is better for this image that the improvement achieved for SWP 25069, one of the component images in the ITF itself. The improvement for SWP 26437 averages between 2.0 and 2.3. Figure 3 shows the ratio of the S/N ratios for the explicit to implicit geometric correction for SWP 27005, an image with a well-exposed spectrum. The average improvement in this case is 1.2 - 1.7. While this is still an improvement, it is not as large in magnitude as in the case of the flat-field data, and could possibly be completely accounted for by the smoothing which occurs during the geometric correction, and during the resampling to create the line-by-line data. The smoothing introduced by the geometric correction alone increases the S/N ratio by factors of 1.1 to 1.5, depending on the position in the image (Nichols-Bohlin 1988). The method of geometric correction currently used in this analysis employs a bi-linear spatial interpolation, which results in significant smoothing of the data between the fiducials. The amount of the smoothing varies across the image depending on the degree of local distortion that must be removed. The improvement in SWP 27005 spectral data is of the order of that expected from smoothing alone, while the improvement in the flat-field data is too large to be accounted for by smoothing alone. It seems clear from these results, that beam-pulling, the phenomenon in which the read beam is deflected toward areas of relatively large charge compared to the surrounding charge, must play a significant role in misalignment of the ITF with the appropriate pixel in the data images.

The improvement in the S/N ratio of the extracted background fluxes has been similarly shown in Figures 4-6. These figures plot the ratio of the S/N ratios of the explicit goemetric correction to the production processing method (implicit geometric correction) in 6 Å bins, for SWP 25069, SWP 26437 and SWP 27005, respectively. The improvement in the background data is similar for all three images, in contrast to the gross spectral data depicted in Figures 1-3. While the improvement for the background of SWP 27005 is not quite as great as for the flat-field images, they are substantially similar, as opposed to the the gross spectral data for this image which shows approximately 50% less improvement than the flat-field data. The results for the extracted background data are consistent with the hypothesis that beam pulling plays an important role in the misregistration of the spectral data with the ITF, while the background data shows significant improvement from proper ITF registration.

Comparison of Stellar Spectra with Explicit and Implicit Geometric Correction

The research to improve the S/N ratio in IUE data is based in part on the assumption that the photometric correction for each pixel can be more accurately determined and thus misregistration noise reduced. If these goals are accomplished, the extracted spectral data should not only be smoother, but more photometrically accurate. An objective determination of the improved accuracy will be difficult to achieve. However, improvements in S/N ratio will most benefit the detection of faint spectral features, so the identification of predicted spectral features that were previously undetected would verify the utility of improving the S/N ratio by means of improved ITF registration.

Data sets from three objects have been chosen to investigate the nature of the improvement to spectral analysis. AR Lac is a cool star representing an emission line spectrum. Twelve well-exposed spectra were chosen to be processed both with the explicit and implicit geometric correction as described above, and then summed. A spectrum of NGC 2346, a planetary nebula, was also selected for analysis. Finally, two spectra of NGC 4151 were chosen. These 3 objects are not intended to represent a definitive test of the usefulness of the signal-to-noise improvement effort. Further study may reveal other objects which better demonstrate the detection of faint spectral features. Figures 4-7 compare the results of extracting spectra from explicitly geometrically corrected data (top spectrum) vs. implicitly geometrically corrected data (bottom spectrum). The data produced from the explicitly corrected data are clearly smoother in all three cases, and many small features are apparent that are not discernable with certainty in the bottom plots. The crucial question, of course, is, "are these features actual spectral features, or noise patterns in the data which, when smoothed, simulate weak spectral features?". The most improvement appears to be achieved in SWP 25682 and SWP 25695, spectra of NGC 4151, and SWP 25889, spectrum of NGC 2359. These spectra were reduced with an extended source reduction method, which utilizes a pseudo-slit of $15\text{x}\sqrt{2}$ pixel height rather than the $9\text{x}\sqrt{2}$ pixel height used for point source data. This result for the extended source extraction reinforces the conclusion that beam-pulling introduces a significant shift in the presence of a large discontinuity in flux on the image (such as in the presence of a strong, point source continuum). The spectra of NGC 4151 are weakly exposed, and the pseudo-slit includes a good deal of background data. The background data are improved by the use of explicit geometric correction almost to the degree of the UV-flood images, as noted above.

Conclusions

We have shown that the improvement in S/N ratio achieved by proper alignment of the ITF with the data image for the gross spectral data is on the order of 20% to 70%, while the improvement in the extracted background data is larger, closer to 40% to 90%. These results indicate that beam-pulling is an important distortion effect not corrected for by the current geometric correction. Most of the increase in S/N ratio is in the 1200-1600 Å wavelength range. There is some loss of resolution in the data extracted from an explicitly geometrically corrected image, but not as much as with implicitly geometrically corrected data that has been smoothed with a three-point filter.

This analysis has been intended to be a first-approximation of the extent of improvement to IUE data which may be anticipated from the S/N effort. The validity and identification of the faint spectral features is left for the reader. The improvement shown here is certainly a lower limit to the improvement that will finally be achieved. Already, many improved methods of geometric correction and ITF construction are being investigated by the project which will yield hopefully improve on the results presented here.

References

Nichols-Bohlin, J. 1988, IUE Newsletter #36, p. 28.

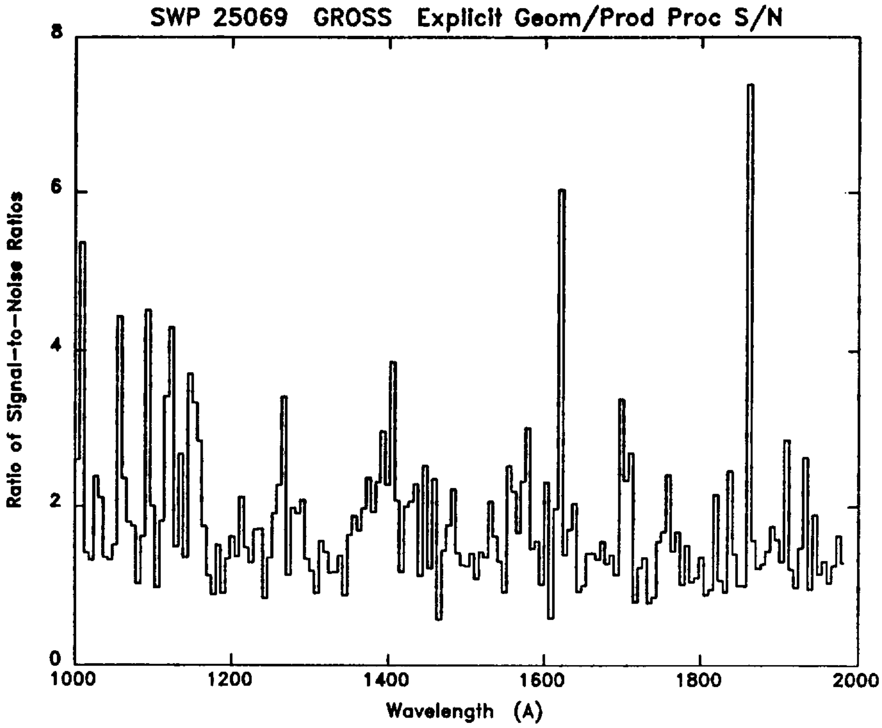

Figure 1: Ratio of the signal-to-noise ratios for gross spectral data of SWP 25069 extracted from explicitly geometrically corrected image vs. production processing method of extraction from an implicitly geometrically corrected image. Data is presented in 6 Å bins.

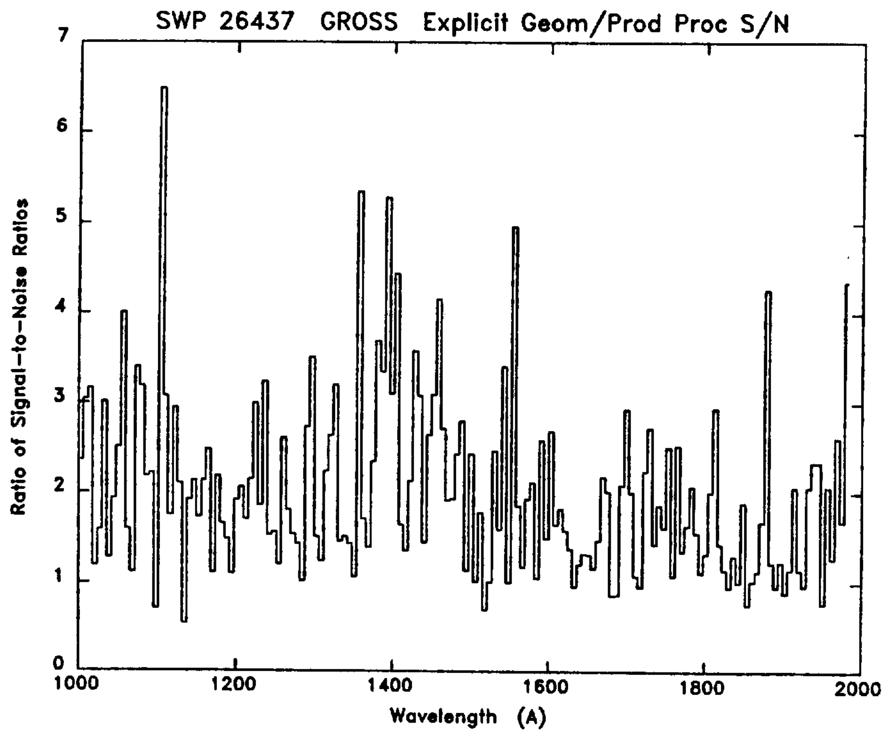

Figure 2: Ratio of the signal-to-noise ratios for gross spectral data of SWP 26437 extracted from explicitly geometrically corrected image vs. production processing method of extraction from an implicitly geometrically corrected image. Data is presented in 6 Å bins.

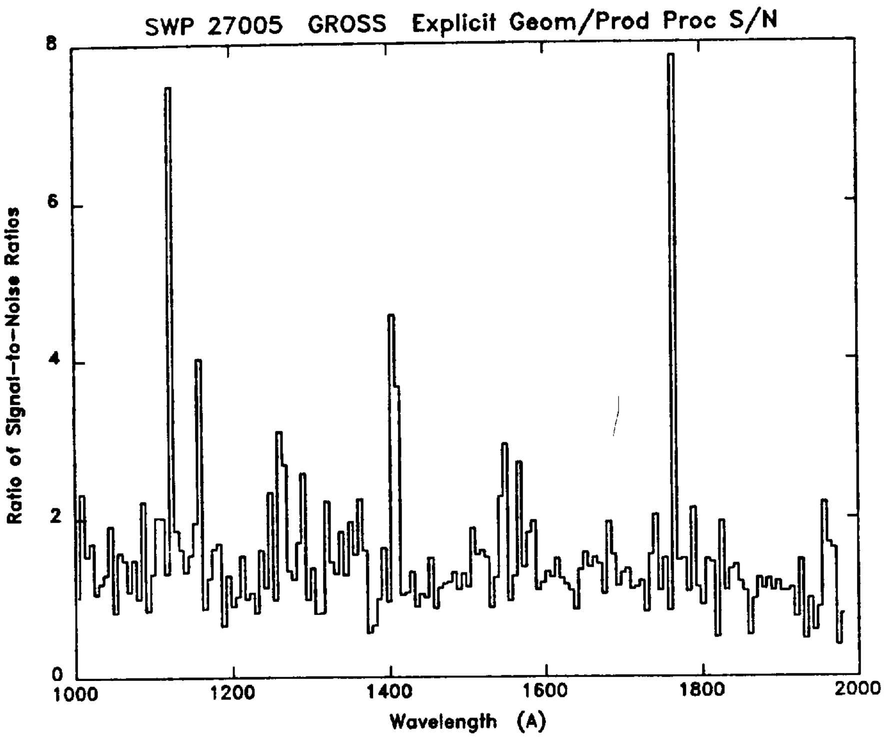

Figure 3: Ratio of the signal-to-noise ratios for gross spectral data of SWP 27005 extracted from explicitly geometrically corrected image vs. production processing method of extraction from an implicitly geometrically corrected image. Data is presented in 6 Å bins.

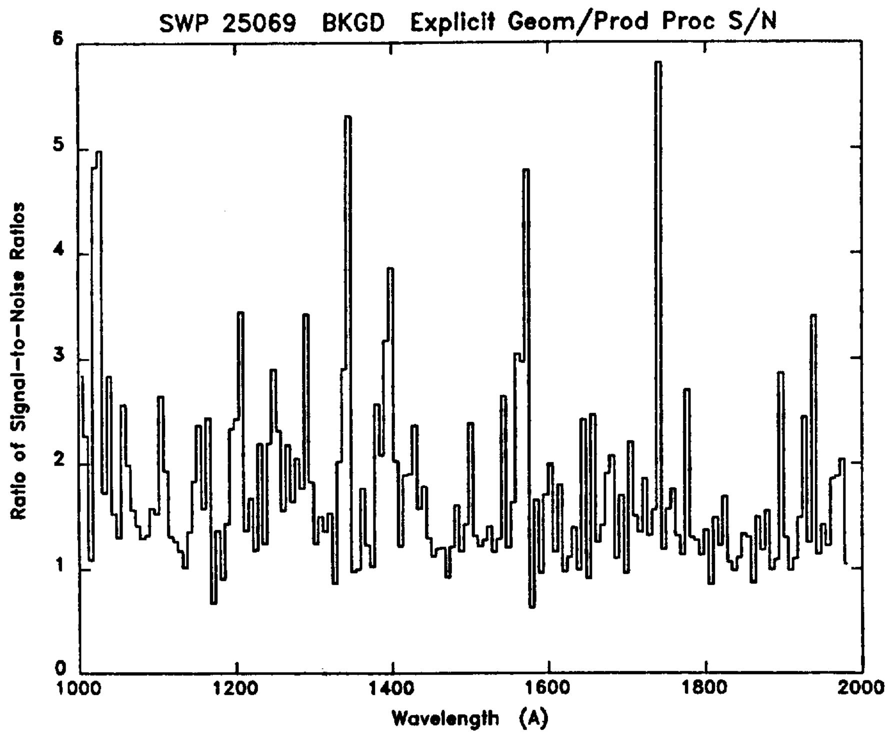

Figure 4: Ratio of the signal-to-noise ratios for background spectral data of SWP 25069 extracted from explicitly geometrically corrected image vs. production processing method of extraction from an implicitly geometrically corrected image. Data is presented in 6 Å bins.

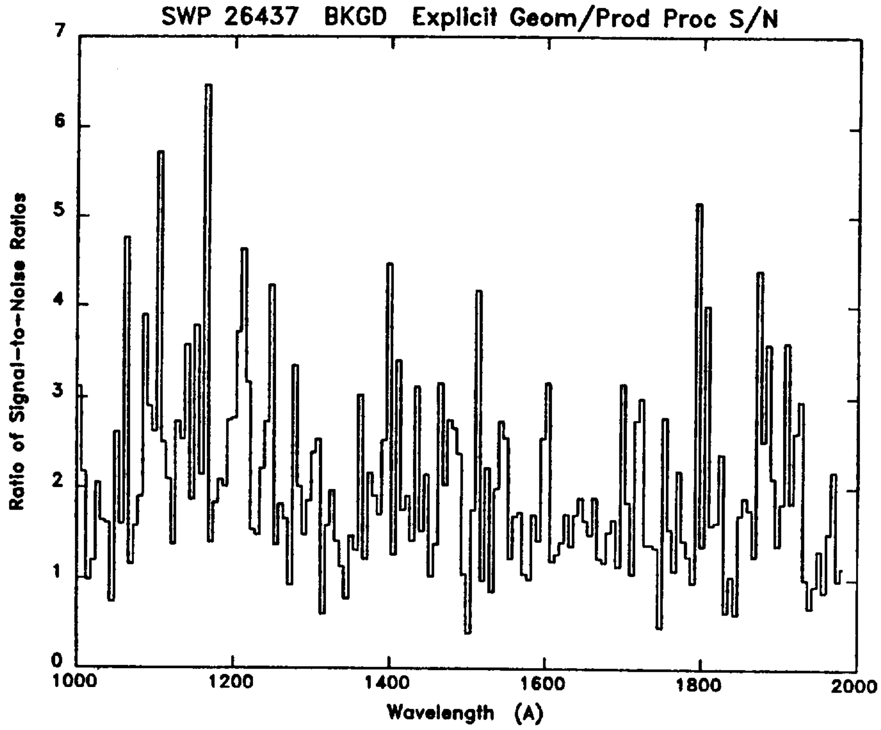

Figure 5: Ratio of the signal-to-noise ratios for background spectral data of SWP 26437 extracted from explicitly geometrically corrected image vs. production processing method of extraction from an implicitly geometrically corrected image. Data is presented in 6 Å bins.

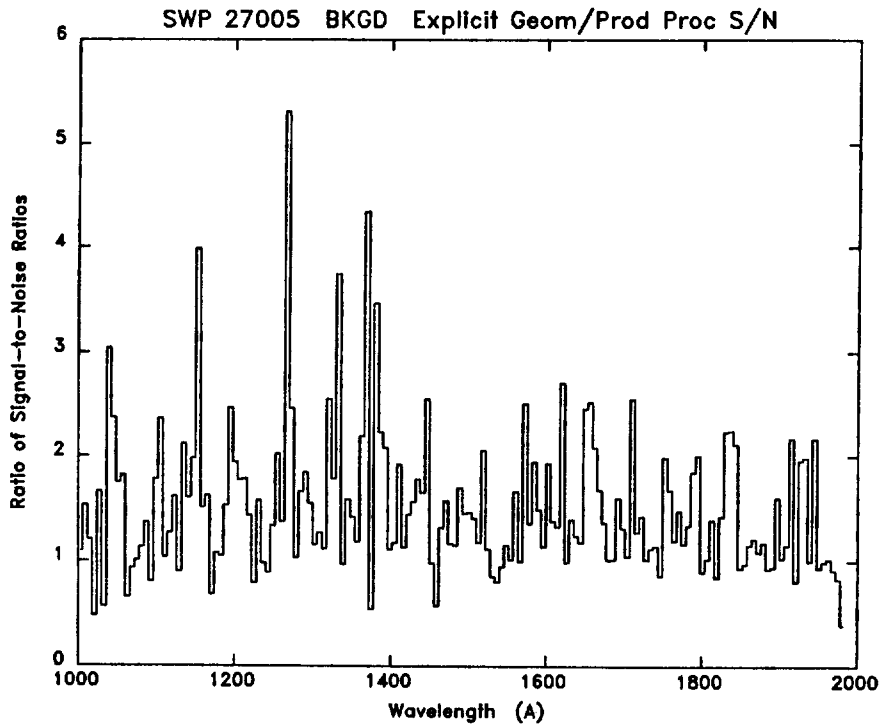

Figure 6: Ratio of the signal-to-noise ratios for background spectral data of SWP 27005 extracted from explicitly geometrically corrected image vs. production processing method of extraction from an implicitly geometrically corrected image. Data is presented in 6 Å bins.

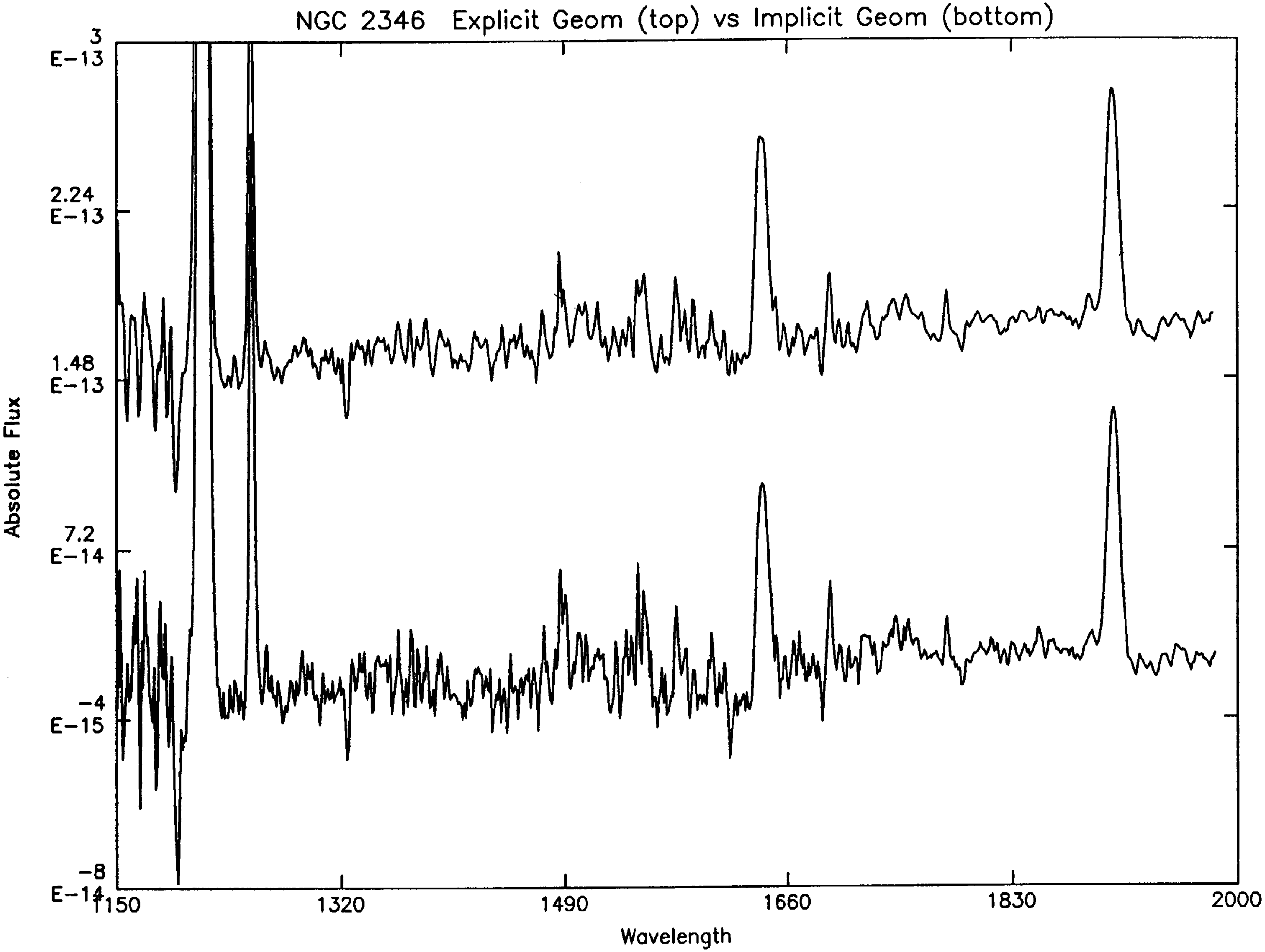

Figure 7: Comparison of extracted spectra of NGC 2346 from explicitly geometrically corrected image (top) and production processing method of implicit geometric correction (bottom). Extraction was performed for an extended source.

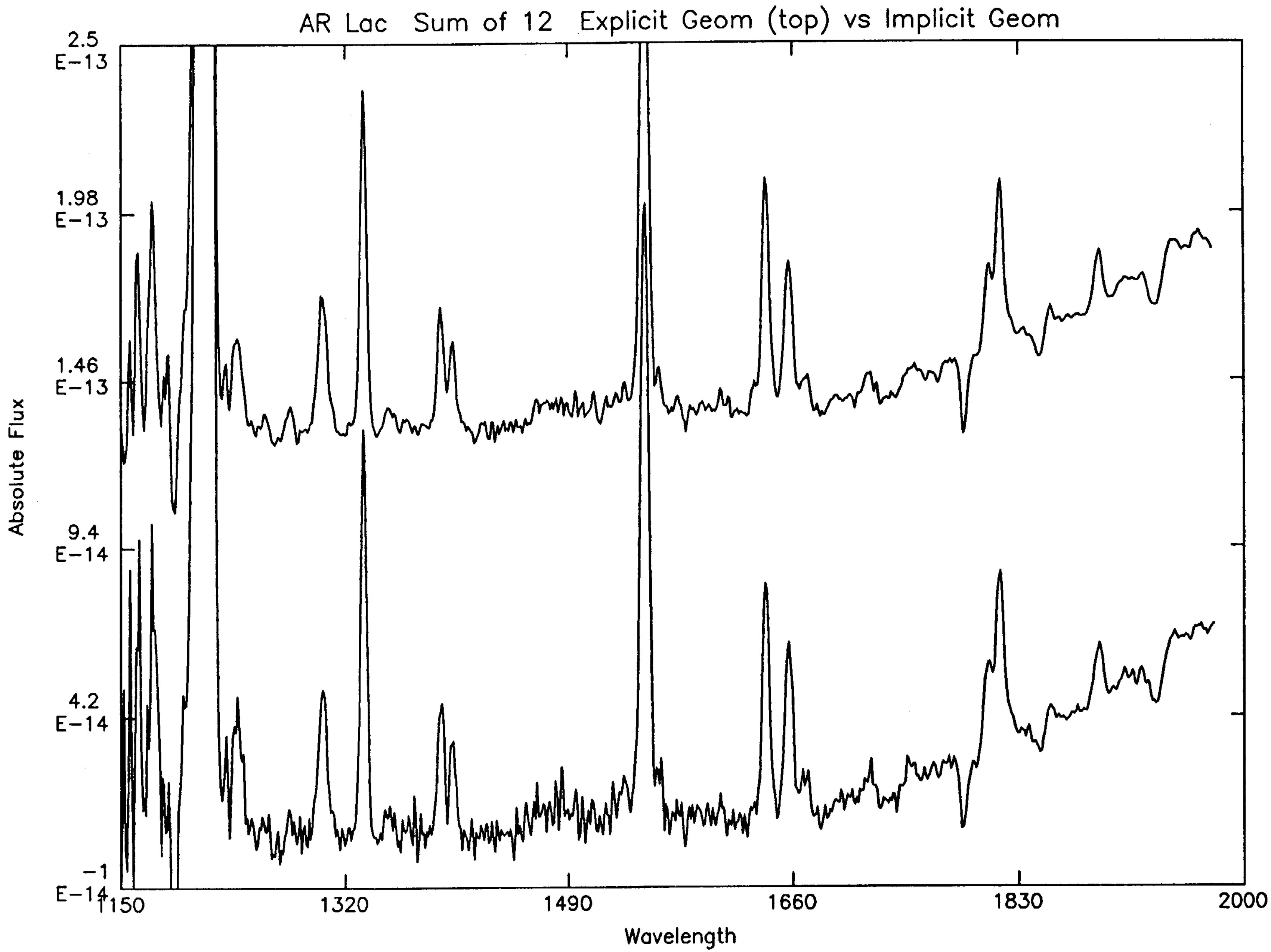

Figure 8: Comparison of sum of 12 extracted spectra of AR Lac from explicitly geometrically corrected image (top) and production processing method of implicit geometric correction (bottom). Extraction was performed for a point source.

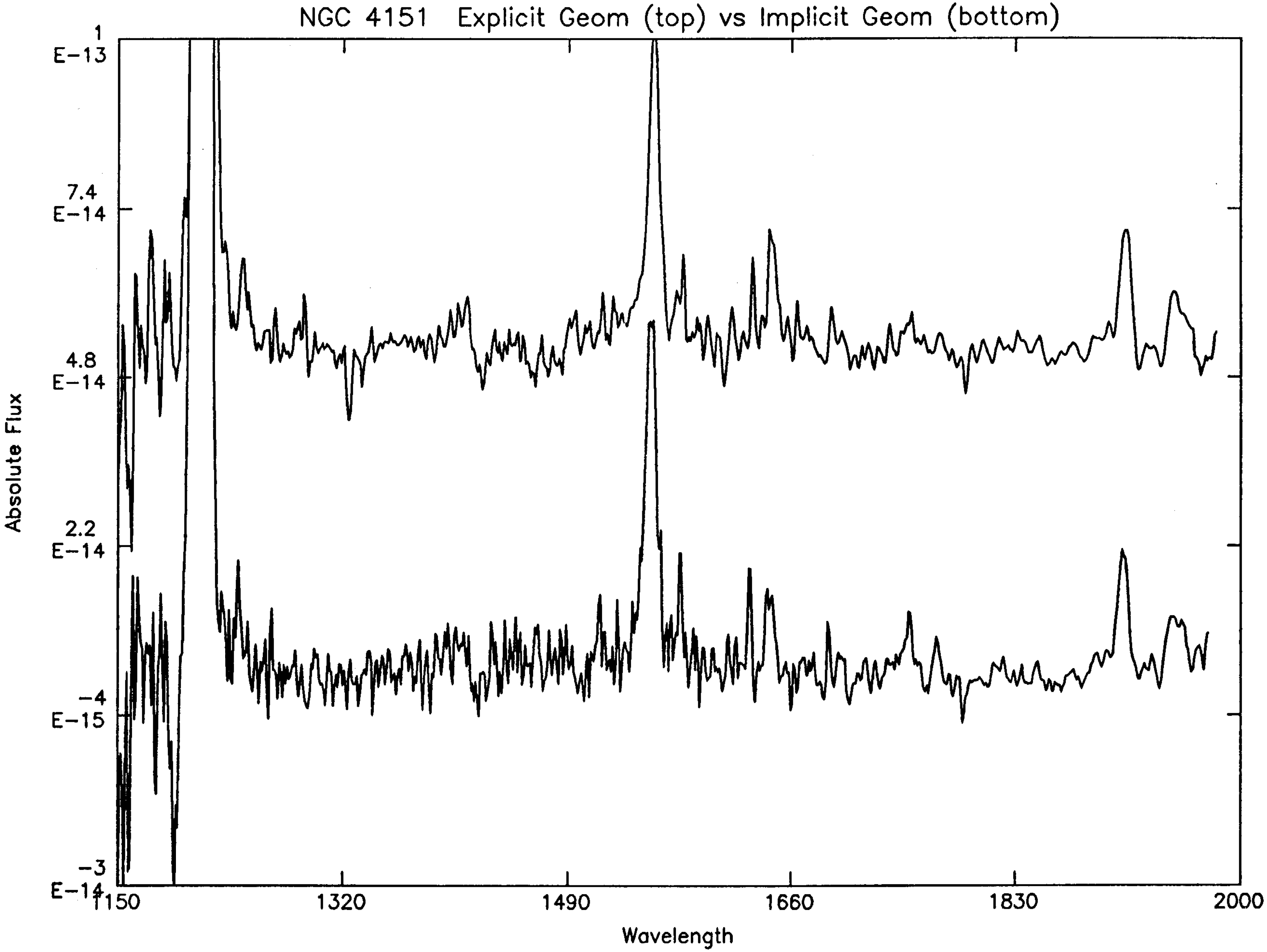

Figure 9: Comparison of extracted spectra of NGC 4151 (SWP 25682) from explicitly geometrically corrected image (top) and production processing method of implicit geometric correction (bottom). Extraction was performed for an extended source.

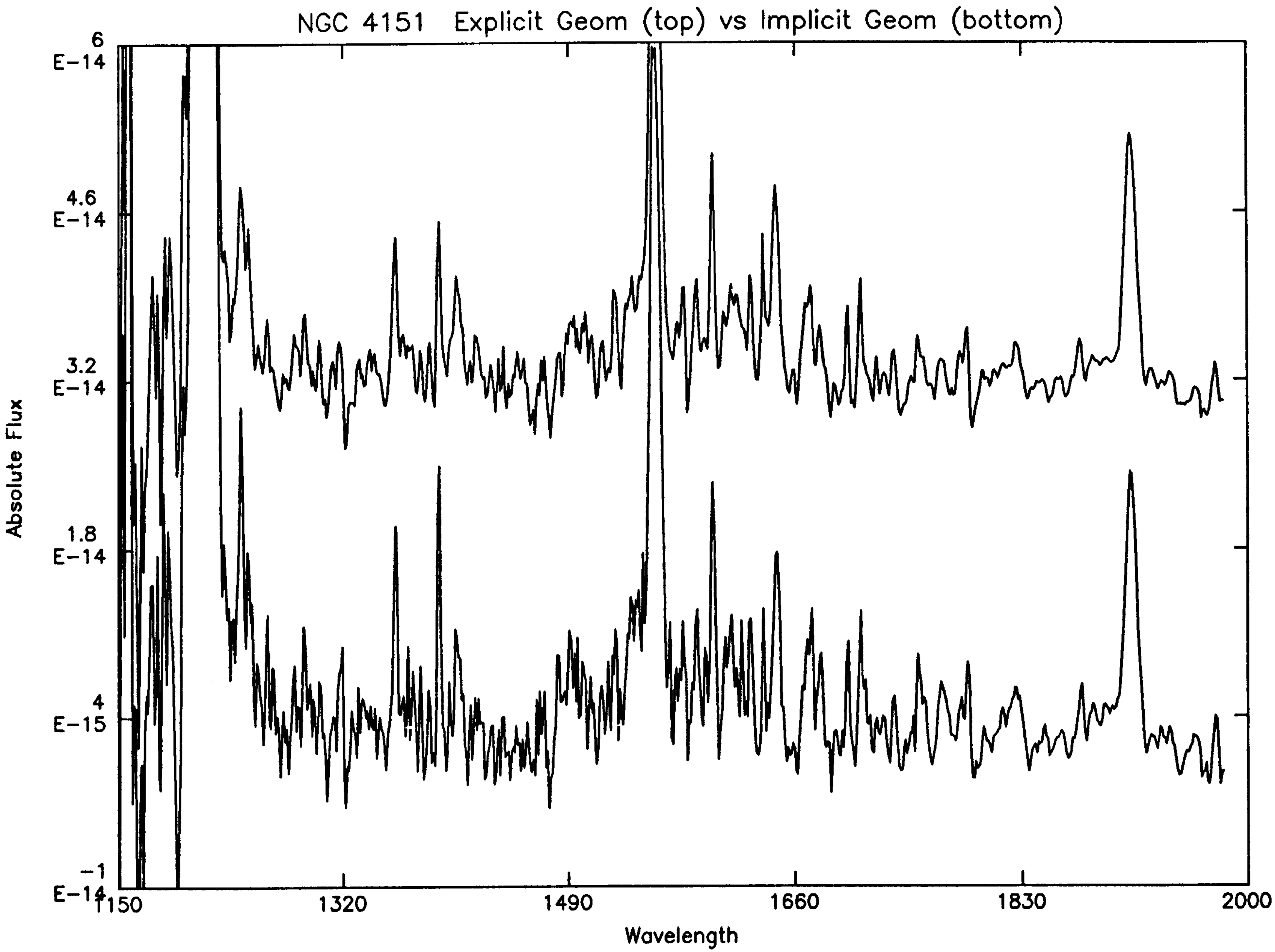

Figure 10: Comparison of extracted spectra of NGC 4151 (SWP 25695) from explicitly geometrically corrected image (top) and production processing method of implicit geometric correction (bottom). Extraction was performed for an extended source.